Accelerating energy release prior to large events in simulated earthquake cycles: implications for earthquake forecasting

Peter Mora and David Place

QUAKES, Department of Earth Sciences, The University of Queensland, Brisbane, Australia (e-mail: mora@earthsciences.uq.edu.au; place@earthsciences.uq.edu.au, phone +61-7 3365 2128; +61-7 33652176, fax: +61-7 3365 7347).

Abstract

Long earthquake sequences are generated using the 2D physically based lattice solid numerical model in a system representing an evolving fracture zone of the Earth's crust subjected to shear. Cycles of seismic activity are observed in which the rate of seismic energy release of simulated earthquakes accelerates in the lead-up to the largest events. During a cycle, the cumulative number of events with energy above a given value is well described by a Gutenburg-Richter power law frequency-size distribution with an exponent similar to earthquake data. The exponent is initially high and becomes low in the latter part of the cycle prior to when the large earthquakes occur. These results indicate that under certain conditions such as those comparable to the model system, earthquake statistics evolve in a predictable way. At least under such conditions, earthquake hazard forecasting would be viable.

Introduction

An ongoing debate in seismology has been whether or not earthquakes are in any sense predictable. One side argues that the power law event-size distributions observed for earthquakes indicate that the earth's crust is in a critical state and hence, a large event may occur at any time (Geller et al., 1997[2]) which implies that prediction is impossible. A counter-argument supported by observational evidence is that at least some parts of the earth's crust are in a critical state only when stress correlations exist in the earth's crust at all length scales within a given region (Jaumé and Sykes, 1999[3]). It is during such periods that it is possible for a rupture to runaway to the largest event size. In this view, the earthquake cycle is proposed to proceed as follows. During the first part of a cycle, small earthquakes occur and re-distribute stress locally. Over time, this process of stress re-distribution allows long-range stress correlations to be established. After this happens, a large earthquake may occur and once it does, the long-range stress correlations will be destroyed and the cycle will repeat. Observations of changes in the frequency-magnitude distribution of earthquakes in the period prior to some large events including the 1989 Loma Prieta earthquake (Jaumé and Sykes, 1999[3]) support this view. Consideration of the earth's crust as a critical system has led various researchers to draw on statistical physics to model seismicity patterns. Sornette and Sammis (1995)[12] showed that if a large earthquake is viewed as a critical point, regional seismic energy release should fit a power law time to failure criterion. Such behavior has been seen in some cellular automaton models such as non-conservative models and/or models with hierarchical fractal cell sizes for seismicity (Sammis and Smith, 1999[11]). Energy release measures such as cumulative seismic moment and Benioff strain have been observed to fit well with a power law time-to-failure function given by $E(t) = A + B(t_f - t)^c$ in a number of cases (Bufe and Varnes, 1993[1]) in agreement with the statistical physics analogy. However, while suggestive, the evidence based on cellular automaton modelling and observational fits of power-law time-to-failure functions do not prove the critical point hypothesis. Nor do the observations prove that earthquake cycles generally exist in which the large events only occur during certain periods which may be identified by analyzing the evolution of earthquake statistics. A realistic physically based numerical simulation model for earthquake activity that reproduces the observed changes in the frequency-magnitude statistics of earthquakes and exhibits accelerating energy release would come a long way towards providing the evidence needed to substantiate the above hypotheses. Such a model would then provide a test-bed for developing an understanding of phenomena such as accelerating energy release and for determining the conditions and statistical characteristics of its occurrence, or for studying general space-time seismicity patterns.

The lattice solid model

The particle-based lattice solid model (Mora, 1992[4], Place and Mora, 1999[10]) has proven successful for modelling fracture processes, fault zone evolution and localisation (Place and Mora, 1999[9]), and has provided a potentially comprehensive solution to the long standing heat flow paradox of seismology (Mora and Place, 1998[7]; Mora and Place, 1999[8]). In the following, long seismicity sequences are studied in a 2D numerical model of a weak zone being subjected to shear (Figure 1). The model consists of two unbreakable solid regions separated by a weak solid region that is allowed to fracture and evolve. The outer edges of the two solid regions are attached to rigid driving plates which are subjected to a normal stress of 150 MPa while being driven in opposite directions at a constant rate of 0.00005 times the compressional wave velocity. This model configuration has been used to represent an evolving fault gouge zone and study the localisation process (Place and Mora, 1999[9]). Here, it represents an evolving fracture zone in the earth's crust. The weak central region is composed of unbreakable groupings of 3 to 10 particles representing blocks of rock. These blocks are arranged in a variety of shapes (triangles, diamonds, hexagons and elongated hexagons). Initially, the blocks are bonded to touching blocks in the weak region by elastic-brittle bonds. These bonds break irreversibly when the separation between touching surface particles exceeds $1.0075R_0$ where R_0 is the particle diameter. Once bonds are broken, touching blocks undergo elastic repulsion and a frictional force opposing slip proportional to the normal force.

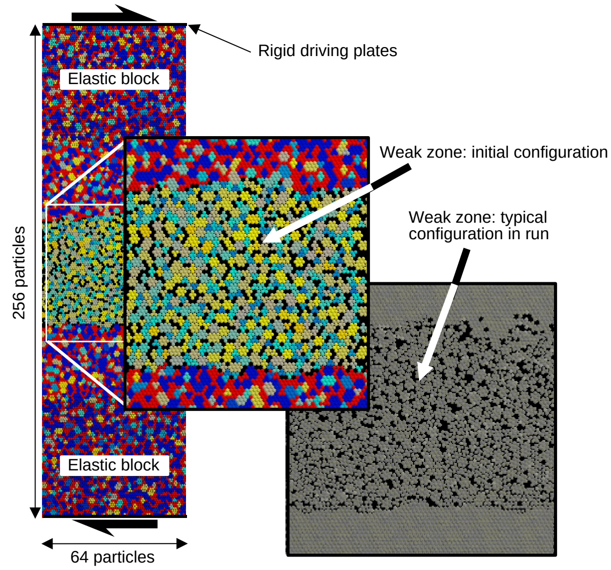

Figure 1: The numerical experimental setup involving a weak layer being sheared. Different shades of grey on the initial configuration plot are used to depict the different strongly bonded blocks. The upper and lower elastic blocks (shown as darker regions) are unbreakable.

As the central weak zone is sheared, the stress builds up. Eventually, the stress is sufficient for bonds to break between blocks. Subsequently, the central zone gradually breaks down and evolves into a steady state defined to be the period when the average rates of bond breaking and cumulative energy release due to simulated earthquakes are almost constant. During most of the numerical experiment, the model gradually deforms as elastic strain energy is building up. When static friction is overcome along any given fracture surface in the model, or if the breaking strength of bonds between different blocks in the weak zone is exceeded, a dynamic slip event may commence. Such slip events in the weak zone represent synthetic earthquakes in the model which release stress and generate seismic waves that propagate away from the rupture surface. These waves are attenuated by an artificial viscosity to avoid kinetic energy buildup in the model that may alter the dynamics of subsequent slip events (Mora and Place, 1994[6]). Hence, kinetic energy in the model increases rapidly during a synthetic earthquake event as stored elastic strain energy is converted to seismic waves during the dynamic rupture event. Once the dynamic rupture event has ceased, kinetic energy dies away gradually as the artifical viscosity attenuates the seismic waves propagating in the model.

Simulated earthquake cycles

A long numerical experiment was conducted in which the system was allowed to evolve into a steady state as defined in the previous section. The kinetic energy is plotted in Figure 2. Each spike on this plot represents a synthetic earthquake. The maxima on the kinetic energy plot approximate the energy release of the synthetic earthquakes. This approximation is good assuming the attenuation is gradual relative to the duration of the dynamic rupture event and provided synthetic earthquakes are well separated in time such that the energy due to previous events has been fully damped out by the artificial viscosity before a new event commences. However, in some cases, this second condition was not met so an algorithm was devised to better approximate the energy release, even when earthquakes are not separated by a long enough time period to avoid superposition of events. In the algorithm, a maximum is taken to indicate a synthetic earthquake. In the period after a maximum while the kinetic energy is decreasing, it is assumed that no further synthetic earthquakes have occurred so the kinetic energy curve should be a decaying exponential of form $\alpha \exp(-\beta t)$. Parameters α and β are determined using least-squares. This allows the assumed functional form for the energy remaining in the model due to the given earthquake to be extrapolated after kinetic energy rises once again due to a new rupture taking place. The difference between the extrapolated decaying form and the kinetic energy of the next maximum is used to approximate the energy of the new synthetic earthquake. The sampling rate was such that a P-wave travels approximately 0.4 particle diameters during one time-step. A 15-point triangular filter was applied to the kinetic energy function prior to application of the picking algorithm to ensure that short time scale dynamic oscillations between kinetic and potential energy are not mistaken for synthetic earthquakes.

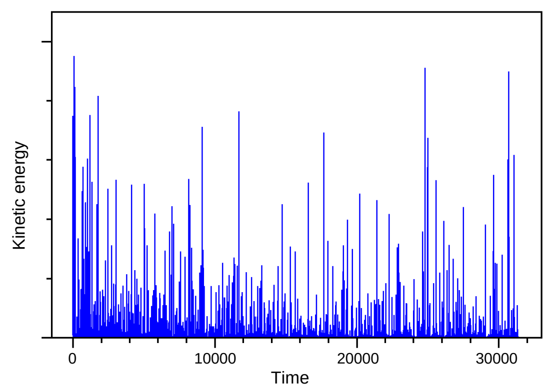

Figure 2: Kinetic energy during the simulation. The time axis is normalised by the time taken for a P-wave to travel 128 particle diameters ~ model size.

Figure 3A shows the cumulative kinetic energy release during the entire simulation. Figure 3B shows a magnification of this curve termed Sequence A during the latter part of the simulation after steady state was reached. During Sequence A, one observes four periods which end with a sharp rise in the cumulative kinetic energy due to the occurrence of large earthquakes. These periods represent synthetic earthquake cycles. In each of these cycles, the sum of square error between the cumulative energy release data and a least-squares linear fit (*EL*) was compared to the square error sum between the data and a least-squares power law time to failure fit (*EP*). The ratio between the square error sums $Q=EL/EP$ is used as a measure of the quality of the power law fit. The numerical value of Q is greater than 1 in three of the four cycles of Sequence A indicating a good fit of the power law time to failure curve in these cases (note: the exponent of the power law curve c was constrained to be negative so $Q < 1$ is possible, c.f. if c is unconstrained, $Q_{min} = 1$).

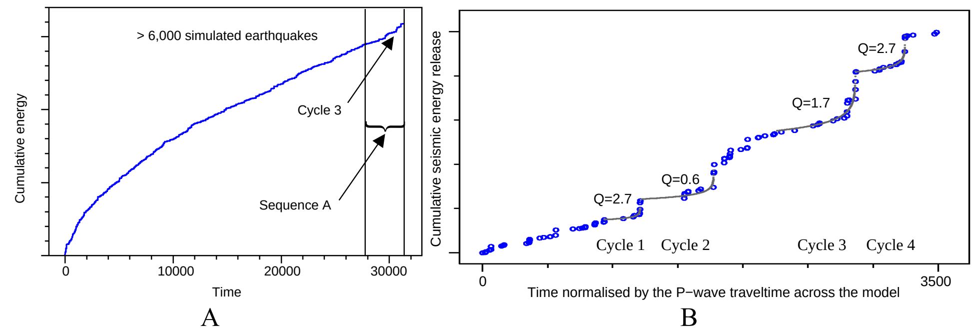

Figure 3: Cumulative seismic energy release. The light grey curves are best fit power law time-to-failure functions computed using least-squares. Numerical values of the power law fit quality factor Q that are greater than 1 indicate the data fits a power law time-to-failure curve better than a straight line.

Evolution of earthquake statistics

The longest synthetic earthquake cycle of Sequence A (Cycle 3) was selected for analysis to study the evolution of earthquake statistics (Figure 4).

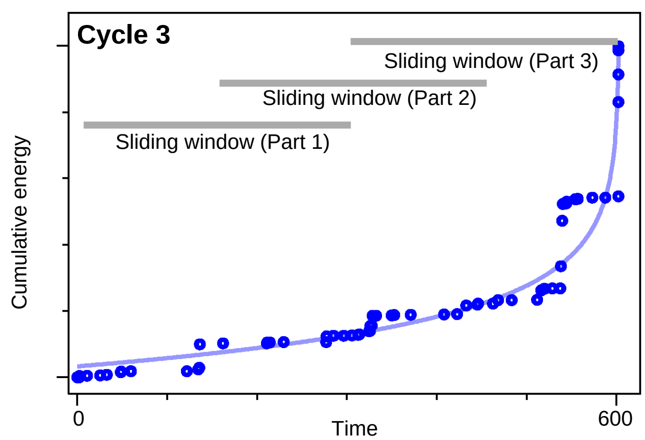

Figure 4: Cumulative seismic energy for Cycle 3 of Sequence A.

In each of three sliding windows labeled Parts 1 through 3 on Figure 4, the statistics of earthquake events were calculated (Figure 5). In Part 1, the curve roughly approximates a straight line corresponding to a power law exponent of $B \sim 1.0$ over nearly 1.5 orders of magnitude. The straight line approximation breaks down at an upper size limit beyond which there is an over abundance of large events relative to the linear fit. In Part 2, again the curve roughly approximates a straight line but only over one order of magnitude. Part 2 has fewer small events than Part 1 but more intermediate to large events, which occur with a greater frequency than the linear fit given on the plot. The slope of the linear fit on the plot corresponds to a power law exponent of $B \sim 0.7$. Finally, in Part 3, the curve well fits a straight line over almost 2.5 orders of magnitude but with a lower power-law exponent ($B \sim 0.4$) than in the earlier parts of the cycle. The power law exponents span the range typically observed in seismically active regions (plate margin or intraplate).

A similar evolution of statistics as in the simulation results has been observed in real earthquake data during the lead up to large events (Jaumé and Sykes, 1999[3]). The initially poor fit to Gutenberg-Richter power law statistics early in the cycle, and excellent fit to Gutenberg-Richter statistics prior to the largest earthquake events supports the critical point model for large earthquakes.

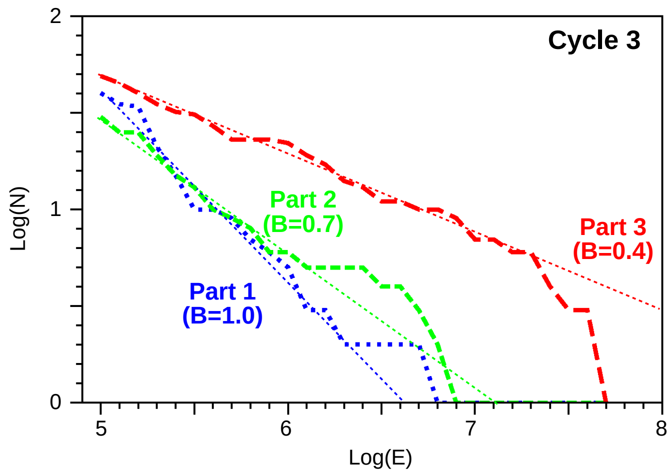

Figure 5: Evolution of earthquake statistics during synthetic earthquake Cycle 3 of Sequence A.

Conclusion

The physically based numerical simulation results indicate that in systems comparable to the model fault system, earthquake statistics can be expected to evolve in a predictable way. The results are in agreement with the critical point model for earthquakes and suggest that regional earthquake forecasting should be viable, at least under conditions similar to the model system.

Acknowledgments

This research was funded by the Australian Research Council, The University of Queensland, and the sponsors of QUAKES. Computations were made on QUAKES' 12 processor Silicon Graphics Origin 2000. P.M. would like to thank Steven Jaumé for suggestions and reviews of a draft manuscript.

References

[1] Bufe., C.G., and Varnes, D.J., 1993, Predictive modeling of the seismic cycle of the greater San Francisco Bay region, J. Geophys. Res., **98**, 9,871-9,833.

[2] Geller, R.J., Jackson, D.D., Kagan, Y.Y., and Mulargia, F., 1997, *Earthquakes cannot be predicted,* Science, **275**, 1616.

[3] Jaumé, S., and Sykes, L., 1999, *Evolving towards a critical point: a review of accelerating seismic moment/energy release prior to large and great earthquakes*, Pure and Appl. Geophys., **155**, in press.

[4] Mora, P., 1992, *A Lattice solid model for rock rheology and tectonics*, The Seismic Simulation Project Tech. Rep. **4**, 3-28 (Institut de Physique du Globe, Paris).

[5] Mora, P., and Place, D., 1993, *A Lattice solid model for the nonlinear dynamics of earthquakes*, Int. J. Mod. Phys. **C 4**, 1059-1074.

[6] Mora, P., and Place, D., 1994, *Simulation of the frictional stick-slip instability*, Pure and Appl. Geophys., **143**, 61-87.

[7] Mora, P., and Place, D., 1998, *Numerical simulation of earthquake faults with gouge: towards a comprehensive explanation for the heat flow paradox*, J. Geophys. Res., **103/B9**, 21,067-21,089.

[8] Mora, P., and Place, D., 1999, *The weakness of earthquake faults*, Geophys. Res. Lett., **26**, 123-126.

[9] Place, D., and Mora, P., 1999, *Numerical simulation of localization phenomena in a fault zone*, QUAKES Tech. Rep. **3**, 227-245 (The University of Queensland, Brisbane).

[10] Place, D., and Mora, P., 1999*, The lattice solid model to simulate the physics of rocks and earthquakes: incorporation of intrinsic friction*, J. Comp. Phys., **150**, 1-41.

[11] Sammis, C.G., and Smith, S.S., 1999, *Seismic cycles and the evolution of stress correlation in cellular automaton models of finite fault networks,* Pure and Appl. Geophys., **155**, in press.

[12] Sornette, D. and Sammis, C.G., 1995, *Complex critical exponents from renormalisation group theory of earthquakes: Implications for earthquake predictions,* J. Phys. I., **5**, 607-619.